JOURNAL OF ELECTROMAGNETIC ENGINEERING AND SCIENCE, VOL. 16, NO. 4, 241~247, OCT. 2016

http://dx.doi.org/10.5515/JKIEES.2016.16.4.241
ISSN 2234-8395 (Online) · ISSN 2234-8409 (Print)

Novel New Approach to Improve Noise Figure Using Combiner for Phase-Matched Receiver Module with Wideband Frequency of 6–18 GHz

Yuseok Jeon* · Sungil Bang

Abstract

This paper proposes the design and measurement of a 6–18 GHz front-end receiver module that has been combined into a one- channel output from a two-channel input for electronic warfare support measures (ESM) applications. This module includes a limiter, high-pass filter (HPF), power combiner, equalizer and amplifier. This paper focuses on the design aspects of reducing the noise figure (NF) and matching the phase and amplitude. The NF, linear equalizer, power divider, and HPF were considered in the design. A broadband receiver based on a combined configuration used to obtain low NF. We verify that our receiver module improves the noise figure by as much as 0.78 dB over measured data with a maximum of 5.54 dB over a 6–18 GHz bandwidth; the difference value of phase matching is within 7° between ports.

Key Words: Amplitude Matching, Broadband Receiver, Front-End, EW System, Phase Matching.

I. INTRODUCTION

Electronic warfare support measures (ESM) systems are required to generate an electronic order of battle. For his purpose, an ESM receiver must intercept emissions from all nearby radars, and measure parameters such as frequency, time-of-arrival, and angle-of-arrival [1].

ESM for electronic intelligence (ELINT) applications places stringent demands on a receiver over a multi-octave bandwidth. Practical solutions must not only meet the electrical specifications but also be compact and immune to microphonic effects and thermal fluctuations. A wideband receiver module was designed to meet these requirements and to provide matching phase and amplitude [2]. A wideband receiver that is located next to an antenna requires low noise figures (NFs) because very low input signals are received by the antenna.

Unfortunately, a low-noise amplifier (LNA) is limited to NF characteristics. Studies have attempted to overcome this limitation by combining two channels. In this case, phase matching between two channels is very important because it can affect the NF.

Fig. 1 shows the block diagram of a wideband receiver with two input channels and one output channel.

A limiter, located in the first stage, is used to protect the receiver module against a high power input signal. If the components in the receiver module are damaged, the module will not operate. A switch between the limiter and the LNA can select the radiofrequency (RF) path or built-in test (BIT) path that

Manuscript received August 12, 2016 ; Revised September 1, 2016 ; Accepted September 6, 2016. (ID No. 20160812-025J)
Division of Electronic and Electric Engineering, Dankook University, Yongin, Korea.
*Corresponding Author: Yuseok Jeon (e-mail: halsuida@naver.com)

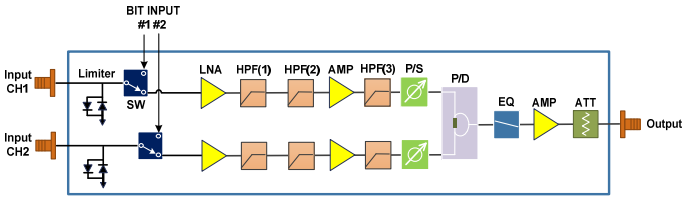

Fig. 1. Block diagram of a wideband receiver with two input channels.

might be used for calibration. A high-pass filter (HPF) is used to eliminate undesirable input signals from the bandwidth. A power combiner is used to combine the two input signals to improve the NF. The phase shifter is for beamforming.

Compared with other receivers, the proposed wideband receiver performs better in terms of NF and phase matching between ports. It was fabricated from 5-mil RT5880 and 10-mil alumina material with gold plating, which can easily be assembled using gap weld bonding.

II. Circuit Topology

To satisfy a system's requirements for the broadband receiver to be located in the front end behind the antenna, the NF, linear equalizer, power divider, and HPF have been considered in the design.

1. Noise Figure

To reduce the NF, a power combiner can be used to combine two input channels. Fig. 2 shows a block diagram for N input signals; the NF can be calculated using Eq. (1). The effective gain ($G_{RF,eff}$) and effective NF (NF_{eff}) are applied to an RF combiner with two N inputs, each having a gain (G_1) and an NF (NF_1) using the conventional two-port definition [3]. In the case of two inputs, the NF can be improved by as much as 0.85 dB using equation 1 if phase matching is perfect.

If there was perfect impedance matching in the combiner cascade, any mismatches would result in a loss of power that would be dissipated in the combiner network.

$$NF_{RF,eff} = \frac{1}{G_{RF,eff}} + \frac{NF_1}{N} - \frac{1}{N^* G_1} \approx \frac{1}{G_{RF,eff}} + \frac{NF_1}{N} \qquad (1)$$

Using Eq. (1), the effective NF ($NF_{RF,eff}$) in Fig. 2 can be calculated where the first term results from the thermal noise generated by the combiner, and the second and third terms result from the noise at the inputs. If the second term is greater than the third, then the NF after combining is reduced by N relative to the NF at the input.

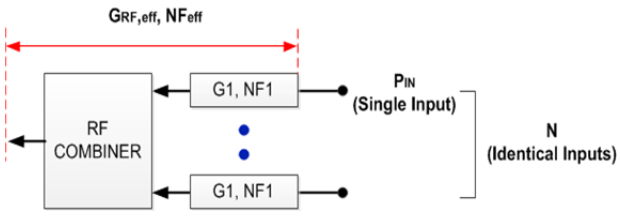

Fig. 2. Block diagram for combination structure of N input signal.

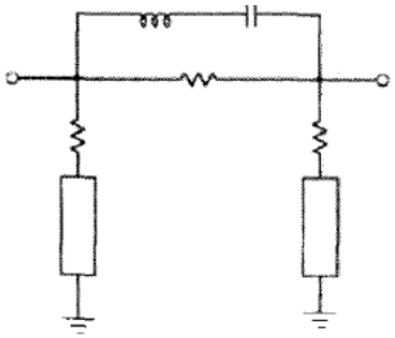

Fig. 3. Basic circuit of linear equalizer.

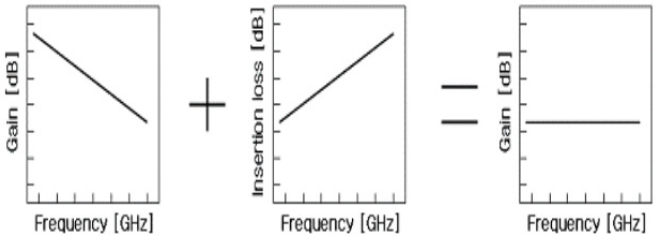

Fig. 4. Diagram showing gain compensation.

2. Linear Equalizer

As shown in Figs. 3 and 4, if a transmission line with a serial resistor is open at a frequency equivalent to the resonance frequency of the inductor and capacitor, the insertion loss ideally becomes zero. The rest of the band is designed to undergo attenuation owing to the T-network of the three resistors, which determines the slope of the line [4].

The broadband receiver tends to end up with increasing overall insertion loss that is attributed to the cascaded placement of dissipative components such as the switch, filter, power divider, and coupler in the wide band RF channel. To achieve the desired quality performance, it is necessary to compensate for the insertion loss with flattening in the gain amplitude over the frequency band of interest. This produced uniform gain performance. The equalizer flattened the amplitude of the resultant insertion loss of the equalizer following the former component over the specified band [5].

3. Broadband Wilkinson Power Divider

The transmission line modeling (TLM) of a two-way equal split Wilkinson power divider (WPD) is shown in Fig. 5. This power divider contains one input port, two quarter-wave transmission lines, two output ports, and one isolation resistor across the output ports.

To increase the bandwidth of the input and output responses

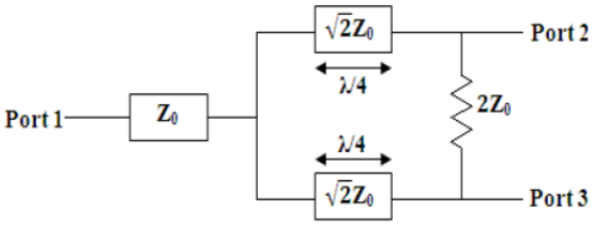

Fig. 5. Transmission line modeling of Wilkinson power divider.

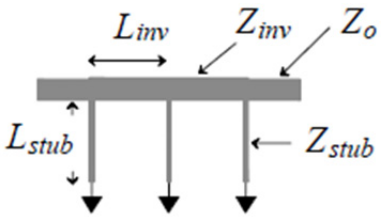

Fig. 6. Geometry of high-pass filter.

of the power divider, a binomial multisection matching transformer is used to minimize the ripple levels. To determine the characteristic impedance, Z_{n+1} of the multisection, beginning with $n = 0$, Eq. (2) is used [6].

$$\ln\frac{Z_{n+1}}{Z_n} = 2^{-N} C_n^{*N} \ln\frac{Z_L}{Z_O}, C_n^{*N} = \frac{N}{(N-n)n} \tag{2}$$

where N is the number of multisections, from 0 to $N-1$, and for a WPD $Z_L = 50\ \Omega$ and $Z_O = 100\ \Omega$.

4. High-Pass Filter

A spurious tone is very important because it a negatively influences signal processing in the total system when unwanted signals come into a broadband receiver. If a spurious tone affects the RF input at low frequency, it creates a harmonic frequency within the operating bandwidth. An HPF is necessary to cancel the spurious tone.

An HPF can be designed as a band-pass filter (BPF) where possible. For the HPF shown in Fig. 6, the ABCD parameters of the impedance inverters and stubs are given by Eqs. (3) and (4), where Z_{inv} and Z_{stub} are the characteristic impedances of the inverter and stub, respectively.

The stub length is determined by choosing $f_o = 12$ GHz, which gives a sufficiently wide passband for our particular design. The passband performance of the HPF depends on the Z_{inv} and Z_{stub} values [6].

The design data of the stub admittances for a maximally flat response can be found where $Z_{inv} = 50\ \Omega$. It is known that the 3 dB point of the HPF, f_{3dB}, is inversely proportional to Z_{stub}.

$$\begin{bmatrix} A & B \\ C & D \end{bmatrix}_{inv} = \begin{bmatrix} \cos\left(\frac{\pi}{2}\frac{f}{f_o}\right) & jZ_{inv}\sin\left(\frac{\pi}{2}\frac{f}{f_o}\right) \\ jY_{inv}\sin\left(\frac{\pi}{2}\frac{f}{f_o}\right) & \cos\left(\frac{\pi}{2}\frac{f}{f_o}\right) \end{bmatrix} \tag{3}$$

$$\begin{bmatrix} A & B \\ C & D \end{bmatrix}_{stub} = \begin{bmatrix} 1 & 0 \\ \frac{-j}{Z_{stub}}\cot\left(\frac{\pi}{2}\frac{f}{f_o}\right) & 1 \end{bmatrix} \tag{4}$$

III. Design and Simulation

The design of the broadband receiver should consider the NF, linear equalizer, power divider, and HPF. The receiver should have the same width to connect different materials and to prevent mismatch. The fabrication is based on the width of the microstrip line of an alumina PCB matched with a microstrip line of a 5-mil RT5880 substrate ($\varepsilon_r = 2.2$) so that they will be interconnected with the alumina and Duroid PCB.

1. Noise Figure

In the combined configuration, the NF was calculated using Eqs. (1) and (2). The combined NF could be improved by approximately 0.85 dB over the NF in a single path. Tables 1 and 2 show how the NF changes in terms of the input signal through a single or combined path.

2. Linear Equalizer

Fig. 7 is based on a PCB material having a dielectric constant of 9.8 and a 10-mil alumina substrate including a thin film resistor (TFR) to reduce the size of the two stages. A 6-18 GHz super-broadband microstrip equalizer was designed according to the resonance and transmission line theory. The transmission line with a serial microstrip line was opened at a frequency equivalent to the resonance frequency (λ/4).

Table 1. Noise figure budget analysis for single path

Broadband Receiver

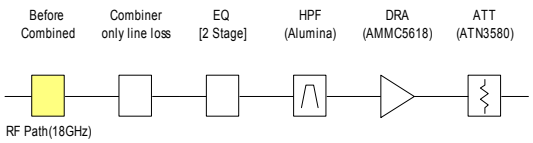

							Total
NF (dB)	4.37	6.00	3.00	1.00	4.30	4.20	5.49
Gain (dB)	15.15	-6.00	-3.00	-1.00	15.80	-4.20	16.75
OP1dB (dBm)	0.85	60.00	60.00	60.00	19.80	60.00	2.45
OIP3 (dBm)	11.69	60.00	60.00	60.00	28.00	60.00	12.92
Input Pwr (dBm)	-30.00	System Temp (K)		290.00			

Table 2. Noise figure budget analysis for combined path

Broadband Receiver

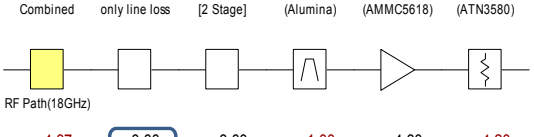

							Total
NF (dB)	4.37	0.00	3.00	1.00	4.30	4.20	4.64
Gain (dB)	15.15	0.00	-3.00	-1.00	15.80	-4.20	22.75
OP1dB (dBm)	0.85	60.00	60.00	60.00	19.80	60.00	8.45
OIP3 (dBm)	11.69	60.00	60.00	60.00	28.00	60.00	17.98
Input Pwr (dBm)	-30.00	System Temp (K)		290.00			

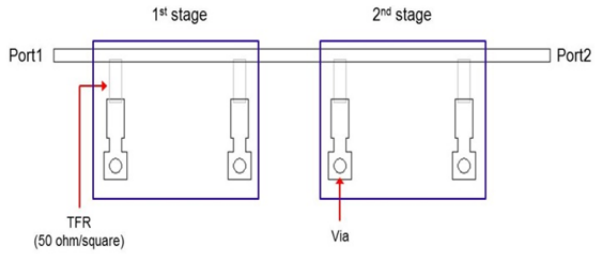

Fig. 7. Momentum of equalizer.

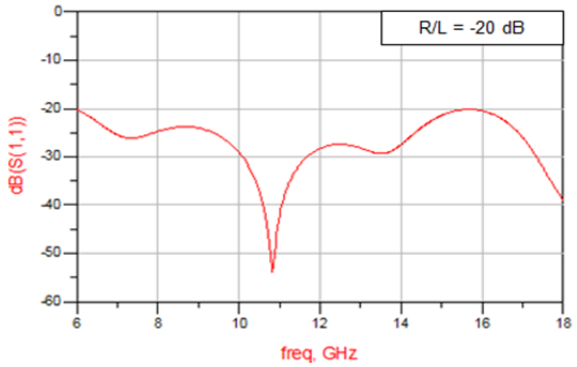

Fig. 8. Simulation result of return loss.

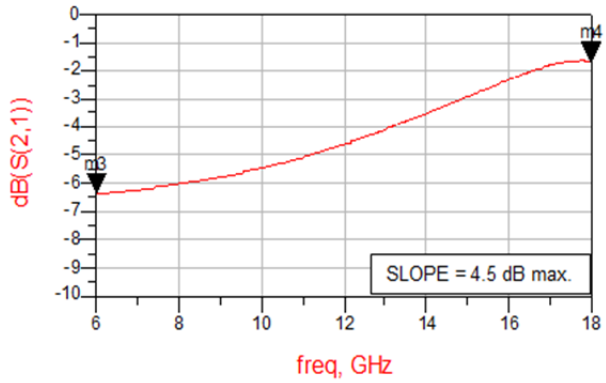

Fig. 9. Simulation result showing the gain slope.

Figs. 8 and 9 show that the input reflection coefficient is a maximum of −20 dB and the amplitude slope is approximately 4.5 dB. The slightly nonlinear behavior seen at 18 GHz arises from the parasitic capacitance of the TFR and transmission lines.

3. Broadband Wilkinson Power Divider

The geometry of a three-stage WPD with in microstrip configuration is shown in Fig. 10. P1 is used to feed the linear equalizer, and P2 and P3 connect RF channels 1 and 2 by gap weld bonding.

A PCB material with a dielectric constant of 9.8 was used with a 10-mil alumina substrate including a TFR that comprised three stages. The characteristic impedance of the λ/4 line at the center frequency of 12 GHz is determined using Eq. (2), where R1, R2, and R3 are the isolation resistors of the multisections as shown in Table 3.

Table 3. Resistor values of three-stage Wilkinson power divider

	R1	R2	R3
TFR value (Ω)	100	210	400

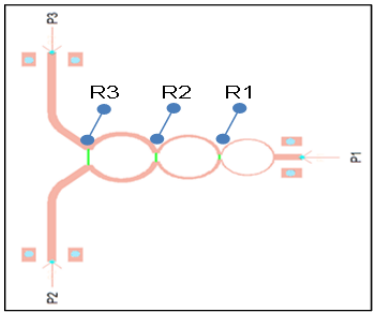

Fig. 10. Momentum of Wilkinson power divider.

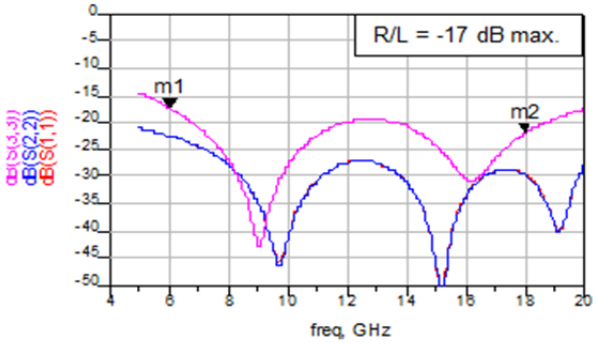

Fig. 11. Simulation result of Wilkinson power divider (return loss).

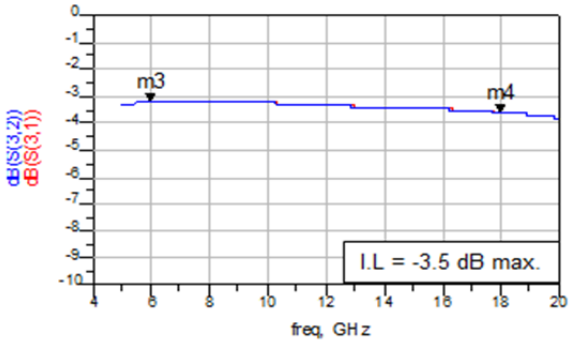

Fig. 12. Simulation result of Wilkinson power divider (insertion loss).

Fig. 11 shows that the input reflection coefficient at each port is a maximum of −17 dB, and Fig. 12 shows that the insertion loss is about around −3.5 dB.

4. High-Pass Filter

The HPF shows a periodic response owing to its distributive nature. It acts as a BPF from DC to 2 f_o. The center frequency f_o should be large enough for the passband performance of the composite BPF to not be destroyed by the notch of the HPF at 2 f_o. Fig. 13 shows the geometry of the HPF with seven poles in

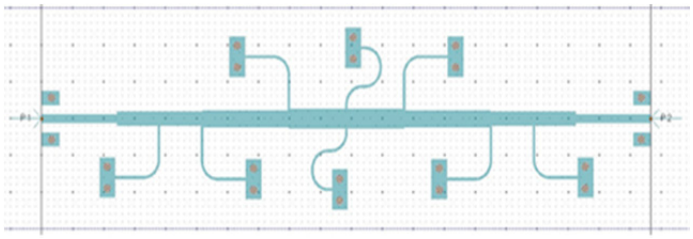

Fig. 13. Momentum of high-pass filter.

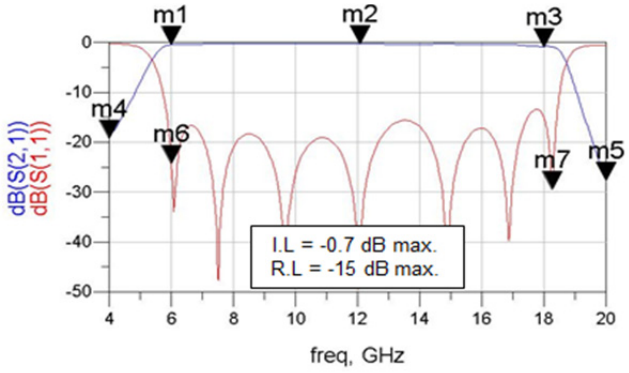

Fig. 14. Simulation result of high-pass filter.

the microstrip configuration. The designed HPF has two holes at each stub to reinforce the grounding effect. The alumina substrate has a dielectric constant of 9.8 and a height of 10-mil.

Fig. 14 shows the performance over a bandwidth where the return loss is −15 dB and the insertion loss is −0.7 dB over 6–18 GHz. The rejection value at 4 GHz is around −18 dB and it can be assumed to be −54 dB after cascading over three HPFs.

IV. Fabrication and Measurement

A GaAs MMIC chip was mounted on a gold-plated substrate to provide good grounding. A high-frequency Duroid PCB was placed around the chip to connect the DC bias, and input and output lines were wire bonded.

Special attention was paid to minimize the length of the wire bonds at the RF signal and ground line [7]. The manufactured wideband receiver comprised a limiter, HPF, power combiner, equalizer, and amplifier. Fig. 15 shows the fabricated module of

Table 4. PCB and active component lists

Section	Details
1. RF PCB material	RT5880 5-mil substrate (dielectric constant: 2.2)
2. Limiter	MMIC based on PIN-diode
3. SPDT and AMP component	GaAs MMIC (bare type)
4. HPF, power combiner and equalizer	Based on microstrip line, alumina 10-mil substrate (dielectric constant: 9.8)

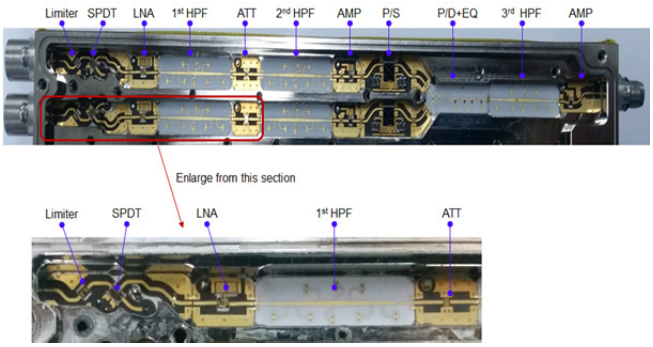

Fig. 15. Broadband receiver with two input channels and one output channel.

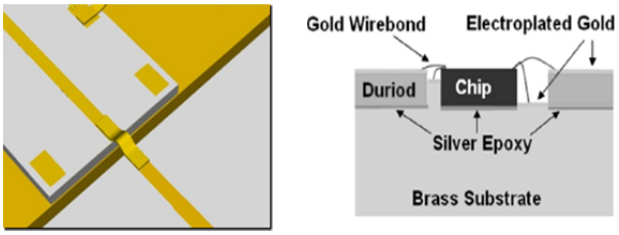

(a) (b)

Fig. 16. (a) Gap weld bonding between alumina and alumina. (b) Wire bonding between MMIC and Duroid substrate.

the broadband receiver with two input channels and one output channel.

Table 4 summarizes the materials used in the receiver. The length of the wire bond needs to be considered when assembling the receiver to ensure phase matching.

Fig. 16(a) and (b) show how different PCBs are connected using gap weld bonding and the MMIC chip and Duroid substrate, by wire bonding.

Figs. 17 and 18 show the measured gain and noise figure in a single path. The gain is more than 17 dB and, the NF improves to a maximum of 5.54 dB in the 6–18 GHz band, respectively. In comparison with the simulated and measured result based on Table 1 and Fig. 18 in the single path, the measured result is approximately equal to the simulated result, being difference by

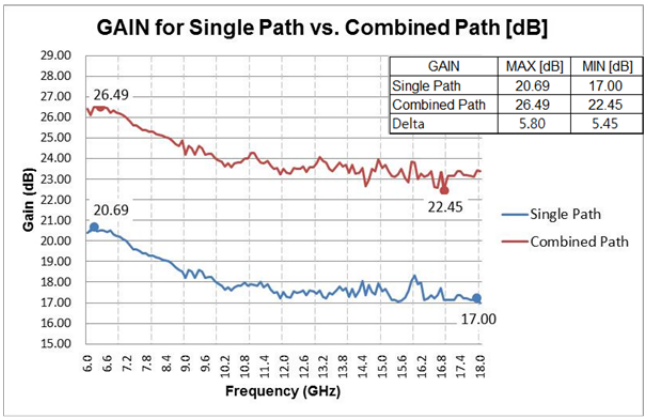

Fig. 17. Measurement result for gain.

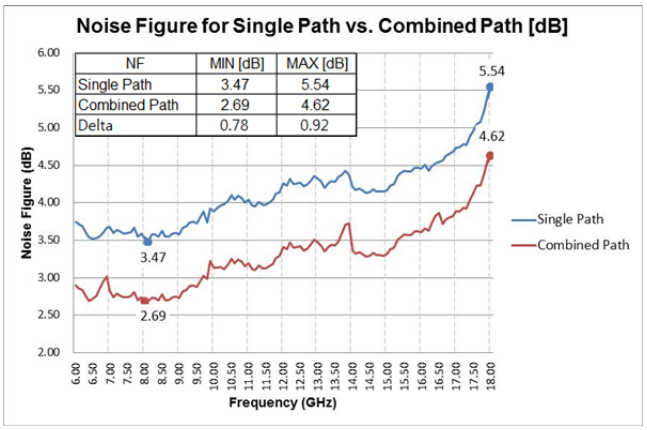

Fig. 18. Measurement result for noise figure.

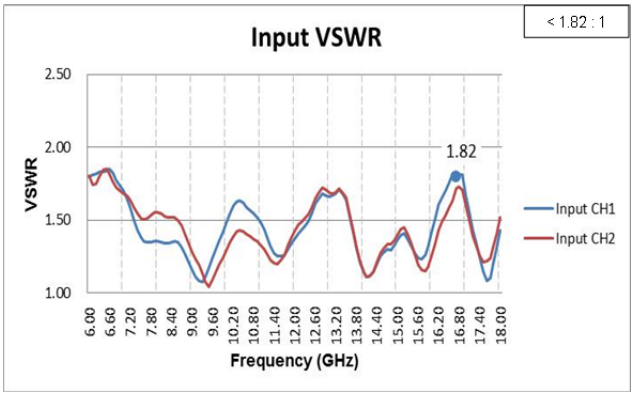

Fig. 19. Voltage standing wave ratio for input of each port.

only 0.05 dB.

A combined noise figure can be calculated using Eq. (1). The NF is approximately 0.78 dB less than that for a single path. A voltage standing wave ratio (VSWR) for the input of each port is shown in Fig. 19. The results are less than 1.82:1 over the 6–18 GHz bandwidth.

The rejection value for 4.5 GHz in the module is approximately 60 dB after cascading through three HPFs, as shown in Fig. 20. An HPF was designed to reject undesirable spurious tones at low frequency. Fig. 21 shows the value of phase matching (7°), and Fig. 22 shows the value of amplitude matching (0.7 dB p-p).

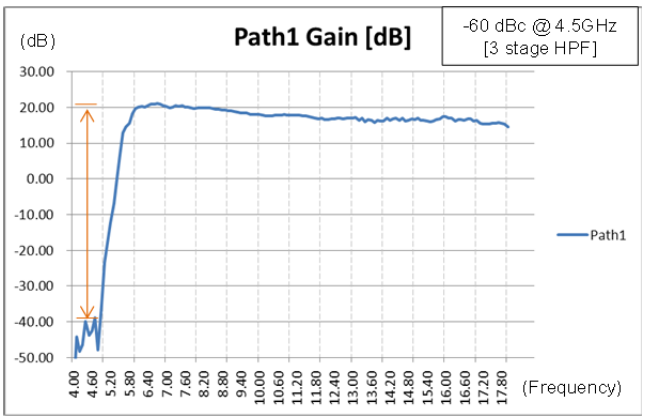

Fig. 20. Measurement of rejection value.

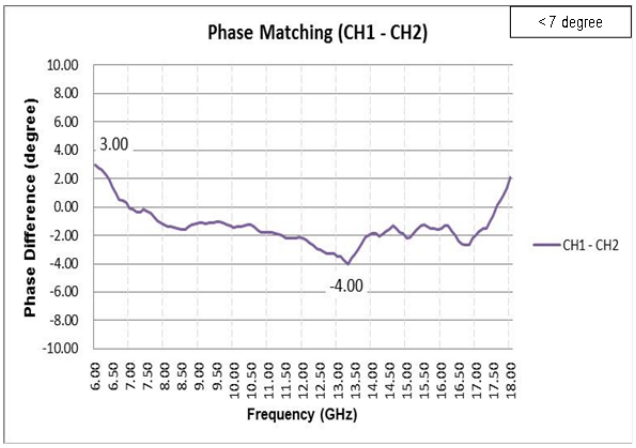

Fig. 21. Measurement result for phase matching.

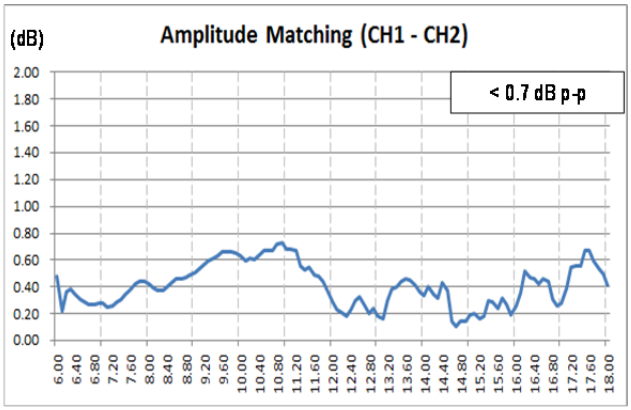

Fig. 22. Measurement result for amplitude matching.

Figs. 21 and 22 prove that the components were operating properly and that the same bonding length, for both wire bonding and gap welding, was used in each RF channel.

V. Conclusion

This paper proposes a 6–18 GHz front-end broadband receiver module with two input channels and one output channel. This high-performance broadband receiver has low NF and good phase matching, making it ideal for ESM applications. A broadband receiver based on a combined configuration can be used to achieve low NF.

We conclude that our receiver module significantly improves the noise figure by as much as 0.78 dB over the measured data with a maximum value of 5.54 dB over the 6–18 GHz bandwidth. In addition, the difference value of phase matching is within 7° between ports.

In the future, this receiver module could be implemented for ESM applications to improve the NF and phase matching performance.

This work was conducted by the research fund of Dankook University in 2015.

REFERENCES

[1] T. N. Tuma, "High temperature superconductivity (HTS) and its role in electronics warfare," in *Proceedings of Avionics Panel Symposium*, Ankara, Turkey, 1993.

[2] L. M. Devlin, G. A. Pearson, A. W. Dearn, P. D. L. Beasley, and G. D. Morgan, "A 2-18 GHz ESM receiver front-end," in *Proceedings of the 32nd European Microwave Conference*, Milan, Italy, 2002.

[3] N. M. Froberg, E. I. Ackerman, and C. H. Cox, "Analysis of signal to noise ratio in photonic beamformers," *in Proceedings of the IEEE Aerospace Conference*, Big Sky, MT, 2006.

[4] B. Mishra, A. Rahman, S. Shaw, M. Mohd, S. Mondal, and P. P. Sarkar, "Design of an ultra-wideband Wilkinson power divider," in *Proceedings of 1st International Conference on Automation, Control, Energy and Systems (ACES)*, Hooghly, India, 2014.

[5] S. Kahng, "Developing the 150%-FBW Ku-band linear equalizer," in *Advanced Microwave and Millimeter Wave Technologies*. Croatia: InTech Europe, 2010.

[6] C. L. Hsu, F. C Hsu, and J. K. Kuo, "Microstrip bandpass filters for ultra-wideband (UWB) wireless communications," in *Proceedings of IEEE/MTT-S International Microwave Symposium Digest*, Long Beach, CA, 2005.

[7] H. Hashemi, X. Guan, A. Komijani, and A. Hajimiri, "A 24-GHz SiGe phased-array receiver-LO phase-shifting approach," *IEEE Transactions on Microwave Theory and Techniques*, vol. 53, no. 2, pp. 614-626, 2005.

Yuseok Jeon

received his B.S. in Electronic Communication Engineering from Cheongju National University, Cheongju, Korea, in 2000 and his M.S. in Electronic Engineering from Chungbuk National University, Cheongju, Korea in 2004. He is currently pursuing his Ph.D. degree in electronic and electric engineering at Dankook University, Yongin, Korea. From 1999 to 2015, he worked with Broadern Inc., Hwaseong, Korea. His research interests include the development of transceivers, receivers, and synthesizers using chip and wire processes for EW and radar system applications.

Sungil Bang

received his B.S. in Electronic Engineering at Dankook University, Seoul, Korea in 1984, his M.S. in Electronic Engineering at Dankook University, Seoul, Korea in 1986, and his Ph.D. in Electronic Engineering at Dankook University, Seoul, Korea in 1992. From 1994 to 1997, he worked as the Director of the research division at LC Tech Inc., Anyang, Korea. Since 1994, he has been a Professor of Electronic and Electric Engineering at Dankook University, Yongin, Korea. His research interests include RF Amp, UWB, OFDM, and RFID for telecommunication applications.